Synthesis and ligand metathetical reactions of supported transesterification catalyst models

J. Schwartz *, S.L. Bernasek, G. Lu, J.P. Keegan, K. Purvis, S. VanderKam

Department of Chemistry, Princeton University, Princeton, NJ 08544, USA

Abstract

Surface-bound complexes of zirconium, titanium, or tin were prepared on hydroxylated aluminum metal in either ultrahigh vacuum (UHV) or under near ambient conditions. Ligand metathetical reactions were performed on these complexes using phenols or carboxylic acids. Reactions were monitored by FT-IR, X-ray photoelectron spectroscopy and temperature programmed desorption in UHV, and by FT-IR and quartz crystal microbalance measurements under near ambient conditions. Ester adducts of surface tin and zirconium alkoxides were observed in UHV, and a tin transesterification catalyst was prepared based on these observations. © 1999 Elsevier Science B.V. All rights reserved.

Keywords: Transesterification; Supported catalysts; Ligand metathesis; Surface tin complexes; Surface zirconium complexes; Surface titanium complexes

1. Introduction

Soluble oxyphilic complexes of Group 4 elements can catalyze transesterification between an alcohol and an ester [1,2]; reaction may occur through a process in which the ester is activated by coordination to the metal. For practical reasons, it was of interest to prepare active heterogeneous analogs of these soluble catalysts. Although ultrahigh vacuum (UHV) surface science is often used simply to elucidate details of chemical synthesis of and bonding between a supported complex and a substrate surface, we use data obtained in UHV as a guide for the synthesis of materials under 'near ambient' conditions. We have demonstrated the preparation of covalently bound, functionalized overlayers on surface oxidized metals or oxides by protolytic attachment of labile organometallic reagents via surface hydroxyl group functionality; in particular, metal alkoxide complexes react easily with –OH groups of a variety of substrates to give surface metal alkoxide species. By subsequent ligand metathesis, 'divergent' synthesis of modified surfaces can be effected (Fig. 1): Utilizing simple and readily available materials, it is possible to start with a common surface species and, through subsequent ligand replacement, prepare a broad variety of surface modified materials whose direct synthesis would be impossible or at least diffi-
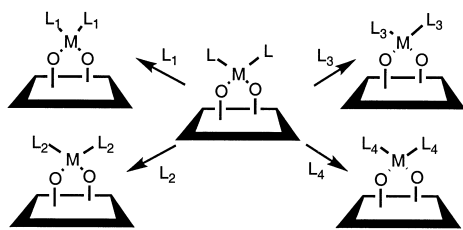
---

* Corresponding author

Fig. 1. 'Divergent' synthesis of surface-modified reagents.

cult to accomplish because of limitations in physical properties of the requisite precursors.

2. Results and discussion

Several oxide-bound zirconium, titanium, and tin alkoxide complexes were prepared in UHV or under 'near ambient' conditions on oxidized aluminum. Replacement of *tert*-butoxy ligands by phenoxides and carboxylates was studied both in UHV and under 'near ambient' conditions for Zr, Ti and Sn species. Ligand metathesis procedures were elucidated using infrared and X-ray photoelectron spectroscopies (XPS), by thermal desorption studies, and by quartz crystal microbalance (QCM) measurements. In all cases, metathesis is apparently driven by the greater acidity of the phenol or carboxylic acid compared with *tert*-butanol. In a parallel investigation, the reaction between surface-bound *tert*-butoxy-Zr and Sn species and simple alkanecarboxylic esters was investigated as a direct model for transesterification.

2.1. Synthesis and characterization of surface alkoxyzirconium or titanium complexes in UHV

The surface hydroxyl group coverage on Al(110) can be controlled through cycles of adsorption of molecular water (170 K) and thermal desorption (300 K) [3]. The thermal decomposition profile for the chemisorptive product of organometallic chemical vapor deposition (OMCVD) of tetra(*tert*-butoxy)zirconium (**1**) on hydroxylated Al(110) in UHV depends on the initial surface –OH group coverage [4]. Deposition of **1** on lightly hydroxylated Al(110) at 170

K, followed by desorption of the multilayer of **1**, gave $[Al^{110}]$–[O]–Zr(*tert*-butoxy)$_3$ (**Al^{110}-2**; XPS, C/Zr = 12.6 ± 0.5; expected C/Zr = 12) formed by protolytic loss of one alkoxy ligand. FT-Reflectance absorbance infrared spectroscopy (FT-RAIRS) of this overlayer shows a strong band for $\nu_{C-H} = 2973$ cm^{-1} (and three bands of lesser intensity at lower frequency). These and other peaks observed [5] agree with those of **1** [6]. Desorption and thermolysis were followed by FT-RAIRS, temperature programmed desorption spectroscopy (TDS) and XPS. Thermolysis of **Al^{110}-2** (300–350 K) gives nearly total decomposition to ZrO$_2$ (by XPS, C/Zr ≈ 0); no intermediate zirconium species could be detected. OMCVD of **1** onto –OH group-saturated Al(110) (170 K) followed by multilayer desorption (240–280 K) also gave **Al^{110}-2**. XPS analysis of peak area ratios (Zr$_{3d}$/Al$_{2p}$) of Zr vs. clean Al showed about 3–4 times as much complex chemisorption had occurred on the saturated vs. lightly hydroxylated Al(110) surfaces. Thermolysis at 350–450 K of –OH group saturated surface-bound **Al^{110}-2** did <u>not</u> result in total decomposition, but instead gave a new surface complex, $[Al^{110}]$–[O]$_2$–(*tert*-butoxy)$_2$Zr, (**Al^{110}-3**) (XPS, C/Zr = 8.6 ± 0.5; expected C/Zr = 8), formed by protolytic loss of a second alkoxy ligand from **Al^{110}-2; Al^{110}-3** was stable to ≈ 450 K, above which it decomposed, leaving surface ZrO$_2$. It is important to note that TDS experiments can clearly differentiate between desorption from a multilayer vs. fragmentation–desorption of a chemisorbed species: Only desorption of the intact zirconium alkoxide gives rise to Zr-containing fragments in addition to *tert*-butyl ligand group-derived ones. Completely analogous results were obtained from the reaction between tetra(*tert*-butoxy)titanium (**4**) and saturation hydroxylated Al(110), which gives $[Al^{110}]$–[O]–Ti(*tert*-butoxy)$_3$ (**Al^{110}-2**; M = Ti); XPS, C/Ti = 12.6 ± 0.5; expected C/Ti = 12) and $[Al^{110}]$–[O]$_2$–(*tert*-butoxy)$_2$Zr, (**Al^{110}-3**; M = Ti) (XPS, C/Ti = 8.6 ± 0.5; expected C/Ti = 8) (Fig. 2).
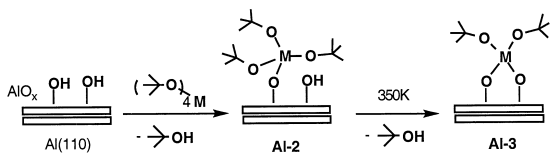
Fig. 2. Deposition of **1** (M–Zr) or **4** (M–Ti) onto heavily hydroxylated Al(110).

2.2. Synthesis and characterization of surface alkoxytin complexes in UHV

Deposition of tetra(*tert*-butoxy)tin (**5**) was accomplished from the vapor phase onto the hydroxylated surface at 170 K. XPS analysis of the resulting multilayer showed C/Sn = 16 (for intact **5**, expected: C/Sn = 16). Desorption of the multilayer was monitored by TDS and RAIRS [4]. Desorption of intact **5** occurred between 220–270 K, but, despite the ostensible similarity between **1** and **5**; the latter reacts with the heavily hydroxylated Al(110) surface in UHV to generate the surface complex with the stoichiometry $[Al]–[O]_3–Sn(OBu^t)$ (**Al^{110}-6**; XPS measured ratio [7–9] C/Sn = 3.7 ± 0.1; expected C/Sn = 4). XPS analysis also showed the presence of a second, minor tin species ($\approx 5\%$ of the total signal) corresponding to Sn(0) [10–12]. In contrast to thermolysis of $[Al]–[O]–Zr(OBu^t)_3$, heating **Al^{110}-6** in the range 300–400 K resulted in complete decomposition (as determined by FT-RAIRS). Surface graphitic carbon (for C_{1s}, BE = 284.6 eV [13,14]), and both oxidized Sn (measured $Sn_{3d5/2}$ BE = 486.5 eV; for SnO_2, BE = 486.5–486.9 eV [7]) and Sn(0) (BE = 484.2 eV [13,14]) were formed. Continued heating above 400 K showed conversion of all the tin to Sn(0), with concomitant loss of surface carbon (by XPS) and evolution of CO (by TDS): Reduction of Sn(IV) to Sn(0) by carbon in this temperature range is possible (Fig. 3). [1,2]

---

[1] Tin metal is prepared by reduction of the oxide with carbon. See Ref. [15].

[2] Reduction of zirconium oxide can be accomplished under forcing conditions using Mg or Ca. See Ref. [16].

2.3. Metathesis reactions of surface alkoxyzirconium complexes with phenols in UHV

Complexes **Al^{110}-2** and **Al^{110}-3** undergo ligand exchange with a variety of phenols, HOC_6H_4X (X = H, CH_3, NO_2, OCH_3) [17], accomplished by cycles of exposure at 170 K followed by warming to 300 K. That simple ligand metathesis and not some other degradation process occurs was demonstrated by XPS analysis. In particular, the XPS-determined atomic ratio of C to Zr measured prior to treatment of **Al^{110}-3** with phenol was C/Zr = 8.2 ± 0.5:1 (expected: 8:1); after four cycles of exposure to phenol, C/Zr = 13.0 ± 0.5 (expected: 12:1), in good agreement with the stoichiometry, $[Al^{110}]–[O]_2–Zr(OC_6H_5)_2$ (**Al^{110}-7**; X = H) (Fig. 4). Further evidence for metathesis was obtained by analysis of the C_{1s} XPS; here, energy resolution is adequate to distinguish C bound directly to O ($BE[C_{1s}] = 287.1$ eV) from C which is bound to C ($BE[C_{1s}] = 285.3$ eV) [8,9]. XPS analysis of the carbon region showed that the atomic ratio of C–O vs. C–C changed from 1:3.6 (expected: 1:3) before phenol exposure to 1:5.4 (expected: 1:5) following ligand metathesis. Qualitative compositional information was also obtained by TDS experiments in which both $m/z = 39$ ($C_3H_3^+$, derived from the benzene ring) and $m/z = 57$ ($C_4H_9^+$, characteristic of the *tert*-butoxy ligand) were monitored during thermal ramp: The appearance of $C_3H_3^+$ began at ca. 400 K (with the desorption peak at ca. 500 K); no signal at $m/z = 57$ was observed over the entire temperature range probed.

Ligand metathesis procedures were also performed using **Al^{110}-2**; exchange occurred more slowly than for **Al^{110}-3**. For the parent phenol,
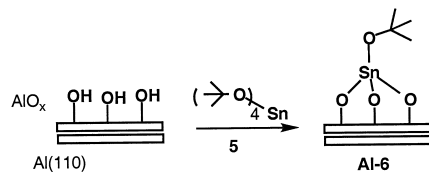

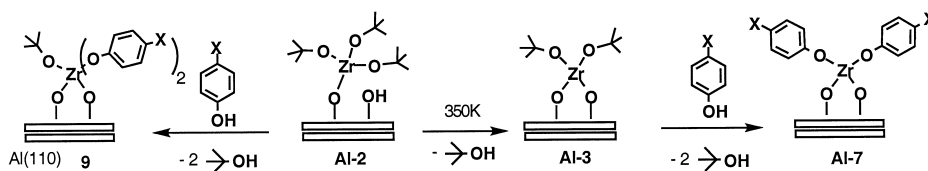Fig. 3. Deposition of **5** onto heavily hydroxylated Al(110).

Fig. 4. Ligand metathesis of $\mathbf{Al^{110}}$-**2** and $\mathbf{Al^{110}}$-**3** with phenols.

eleven cycles of dose (170 K) and removal (300 K) were performed; FT-RAIRS analysis showed that bands characteristic of the *tert*-butoxy ligand (2977 and 1197 cm^{-1}) were still (barely) observable; XPS analysis also showed that nearly complete exchange of phenoxide for *tert*-butoxide had occurred (C/Zr = 18.5 ± .5; expected: 18:1 for $[Al^{110}]–[O]–Zr(OC_6H_5)_3$) ($\mathbf{Al^{110}}$-**8**). Two types of C were observed by XPS (C–O vs. C–C = 1:5.0; expected: 1:5) consistent with phenoxide ligation. Qualitative compositional information was also obtained by TDS experiments for $\mathbf{Al^{110}}$-**8** as was done for $\mathbf{Al^{110}}$-**7**. However, in contrast to the former case, both m/z = 39 ($C_3H_3^+$, derived from the benzene ring) and $m/z = 57$ ($C_4H_9^+$, characteristic of the *tert*-butoxy ligand) were observed during thermal ramp: The appearance of $m/z = 39$ began at ca. 400 K (with the desorption peak at ca. 500 K) and $m/z = 57$ was observed as a sharp peak at 350 K. Noteworthy is the observation that, except when the parent phenol was used with Al^{110}-2, incomplete exchange occurred, consistent with replacement of only 2 *tert*-butoxy ligands to give $\mathbf{Al^{110}}$-**9**. This difference in reactivity from $\mathbf{Al^{110}}$-**3** might be due in part to relatively dense packing of ligand groups in $[Al^{110}]–[O]–Zr(tert\text{-butoxy})_2(\text{phenoxy})$, which impedes further coordination of a phenolic molecule, necessary to complete metathesis. Comparatively, crowding in $[Al^{110}]–[O]_2–Zr(tert\text{-butoxy})_1(\text{phenoxy})$ may not be so acute.

2.4. Metathesis reactions of the surface alkoxytin complex with phenols in UHV

Surface complex $\mathbf{Al^{110}}$-**6** undergoes ligand metathesis with phenol in UHV [18] (Fig. 5).

Following four cycles of dosing (170 K) and desorption (240 K), FT-RAIRS analysis showed complete loss of the *tert*-butoxy group. Although phenoxy for *tert*-butoxy ligand exchange in $[Al]–[O]_{4-n}–Zr(OBu^t)_n$ ($n = 2,3$) can be accomplished with subsequent desorption of unreacted phenol at 300 K, heating no higher than 240 K was attempted for reactions of $\mathbf{Al^{110}}$-**6**, given its thermal lability. After these four cycles, XPS analysis showed two tin species to be present. The lesser component (30% of total signal) corresponded to Sn(0) (apparently formed even below 300 K) and the major component was Sn(IV). The atomic ratio, C/Sn = 6.0, is consistent with simple ligand metathesis to give $[Al]–[O]_3–Sn^{IV}(OC_6H_5)$ ($\mathbf{Al^{110}}$-**10**; expected C/Sn = 6). Thermolysis of $\mathbf{Al^{110}}$-**10** up to 700 K showed complete decomposition to Sn(0) by XPS.

2.5. Synthesis and metathesis reactions of surface alkoxyzirconium complexes with phenols under 'near-ambient' conditions

In a typical metathetical procedure [17], a surface hydroxylated Al substrate [3,4] was treated with vapor of **1**. Protolytic deposition occurred with loss of ca. two alkoxide ligands to give product with an average stoichiometry, $[Al]–[O]_2–Zr(tert\text{-butoxy})_2$ (**Al-3**) [19,20]. The
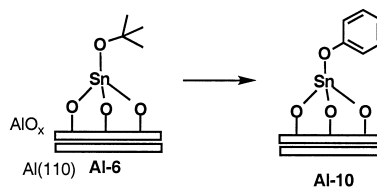

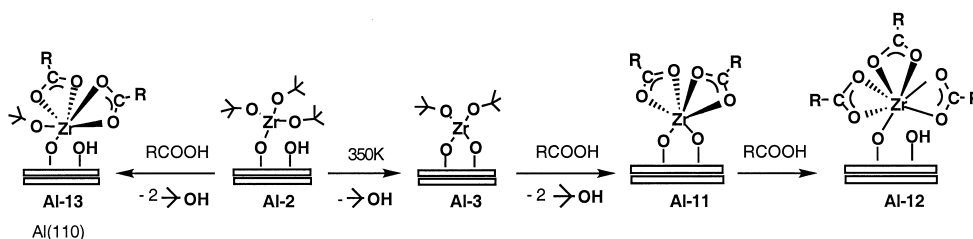Fig. 5. Ligand metathesis of $\mathbf{Al^{110}}$-**6** with phenols.

Fig. 6. Metathesis in UHV to give **11**, **12** and **13**.

substrate was then subjected to four cycles of phenol exposure (10^{-2} Torr) followed by evacuation. Specular reflectance FTIR spectroscopy was used to monitor ligand metathesis; in particular, strong peaks for the *tert*-butoxy ligand (2973 and 1197 cm^{-1}) were reduced in intensity, and peaks corresponding to the phenolic ligands of [Al]–[O]$_2$–Zr(phenoxy)$_2$ (**Al-7**) grew with each exposure cycle.

2.6. Metathesis reactions of surface alkoxyzirconium complexes with alkanecarboxylic acids in UHV

Complete exchange of *tert*-butoxy ligands for carboxylates occurred for **Al^{110}-3** after several cycles of dosing (170 K) and warming (300 K), depending on the acid (Fig. 6) [21]. Ligand metathesis was monitored by RAIRS by noting the disappearance of the band at 1200 cm^{-1}, characteristic of ν_{C-O} for the *tert*-butoxy ligands, and the increase in intensity of bands attributable to carboxylate ν_{sym} and $\nu_{antisym}$ at 1477 and 1600 cm^{-1}, respectively [22,23]. XPS analysis of the metathesis product (**Al^{110}-11a**; R = C$_3$H$_7$) established the stoichiometry of the overlayer to be close to [Al]–[O]$_2$–Zr(O$_2$CR)$_2$ (C/Zr = 9.8 ± 0.3; expected 8). Further exposure to the acid gave [Al]–[O]–Zr(O$_2$Cr)$_3$ (C/Zr = 14.3 ± 0.7, expected 12; **Al^{110}-12a**); one surface O–Zr bond is apparently cleaved by the acid. It is interesting to note that although the same ratio, C/Zr = 8:1, is expected for both **Al^{110}-3** and **Al^{110}-12a**, resolution of the C$_{1s}$ spectrum, focusing on differences between alkoxide carbon ($\underline{C}$–O) of **Al^{110}-3** and carboxyl-

ate carbon ($\underline{C}$(=O)O) of **Al^{110}-12a** [9], easily distinguishes between these ligand types. TDS analysis for the final surface species showed essentially no signal at $m/z = 57$ below 450 K, and confirms the absence of *tert*-butoxy groups. No carboxylate ligand desorption was noted for **Al^{110}-12a** or **Al^{110}-12b** (R = C$_7$H$_{15}$) which were stable to > 500 K. [3]

Only incomplete metathesis was observed for reaction between butanoic acid and **Al^{110}-2** [21]. Even after 12 cycles of dose (170 K) and warm (300 K), bands characteristic of mixed alkoxide (1200 cm^{-1}) and carboxylate (1477; 1600 cm^{-1}) ligation were observed by RAIRS (Fig. 3). Furthermore, TDS analysis for the resulting material (**Al^{110}-13**) showed a significant signal at $m/z = 57$ in the temperature range 300–400 K, characteristic of thermal decomposition of the *tert*-butoxy ligand (Fig. 2) [4,24]. As for **Al^{110}-3** and **Al^{110}-12a**, observed C/Zr ratios for **Al^{110}-2** and **Al^{110}-13** were nearly the same (ca. 12:1). Here, analysis of the deconvoluted C$_{1s}$ XPS signal as a function of butanoic acid dose cycle showed asymptotic replacement of alkoxide ligands by butanoate, and the final stoichiometry [Al]–[O]–Zr(O$_2$CC$_3$H$_7$)$_2$(OC-[CH$_3$]$_3$)$_1$ was established. Incomplete ligand metathesis for **Al^{110}-2**, even after exhaustive cycles of dose and heat as noted for phenols, is attributed to steric factors in which the *tert*-butoxy ligands of **Al^{110}-2** are in a more congested environment than are those of **Al^{110}-3**. In

---

[3] These observations are consistent with estimates of bond energies. See Ref. [24].

this proposal, replacement of two of the three alkoxide ligands of **Al[110]-2** leaves the third alkoxide group sufficiently sterically inaccessible that further metathesis is unlikely.

2.7. Metathesis reactions of surface alkoxyzirconium complexes with alkanecarboxylic acids under 'near-ambient' conditions

The reaction between carboxylic acids and metallic oxide surfaces, particularly of Al, has been studied as a means to attach organic films to oxides [22,25,26], but QCM measurements [5] show that simple alkanoic acids adsorb reversibly onto the oxidized Al surface. However, reaction of the carboxylic acid with **Al-3** enables irreversible subsequent adsorption of the alkanecarboxylic acid by formation of **Al-11** [5]. Infrared analysis of **Al-11** showed the alkane chains are not highly ordered [27], and that the carboxylate ligands were η^2-ligated to Zr [28]. Reaction of **Al-3** with carboxylic acids gives surface-bound species of average stoichiometry [Al]–[O]$_2$–Zr(carboxylate)$_2$ (**Al-7**) [5], determined by QCM measurements [19,29,30]. These surface complexes are inaccessible by direct chemical vapor deposition routes in part because of low volatility of the tetracarboxylate complex precursor [28] and because of the relative acidities of surface –OH groups and the alkanecarboxylic acids.

2.8. Synthesis and metathesis reactions of surface alkoxytin complexes with alkanecarboxylic acids under 'near-ambient' conditions

The reaction between surface hydroxylated aluminum and **5** was monitored by QCM. Fol-

lowing chemisorption and desorption of any multilayer **5**, surface tin complex **Al-6** was exposed to vapor of octanoic acid; ligand metathesis was also followed by QCM. The ratio of QCM frequency changes (2.6:1) effected in this two step synthesis is close to that expected (2.8:1) for the stoichiometry of **Al-6** to be [Al]–[O]$_3$–Sn(*tert*-butoxide), as was determined for the product of chemisorption in UHV. As for Zr and Ti analogs, continued exposure of **Al-14** to octanoic acid resulted in sequential cleavage of surface O–Sn bonds (via **Al-15**), ultimately giving surface adsorbed tin tetracarboxylate. Since chemisorption of **1**, **4** or **5** requires proton transfer to an alkoxide ligand common to all [29,31], structural differences for surface hydroxyl group coordination of **5** vs. **1** or **4** may explain differences in the stoichiometries measured for **Al-2** and **Al-6**. The reaction between a simple alcohol and the metal alkoxides may help elucidate the origin of this difference in surface deposition stoichiometries. Although Sn(OPr^i)$_4$ and Zr(OPr^i)$_4$ adducts with *i*-PrOH are structurally similar di-μ-alkoxy bridged dimers in which each metal is 6-coordinate, average Sn–O distances for monodentate axial (2.12 Å) and monodentate equatorial (1.95 Å) alkoxide ligands are different by only ca. 0.17 Å [32], but for the Zr analog this difference (axial 2.27 Å vs. equatorial 1.93 Å) is ca. 0.34 Å [33]. Significantly, coordination of the alcohol in two of the four *axial* sites of the dimer is indicated; perhaps bonding of the alcohol is stronger to Sn(IV) than to Zr(IV) in these model systems. If so, it may be that **3** binds more strongly than **1** to surface –OH groups of oxidized Al, giving rise to the observed difference in chemisorption stoichiometries (Fig. 7).
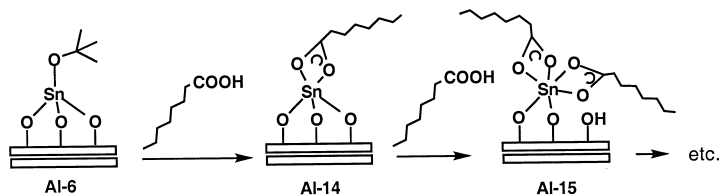

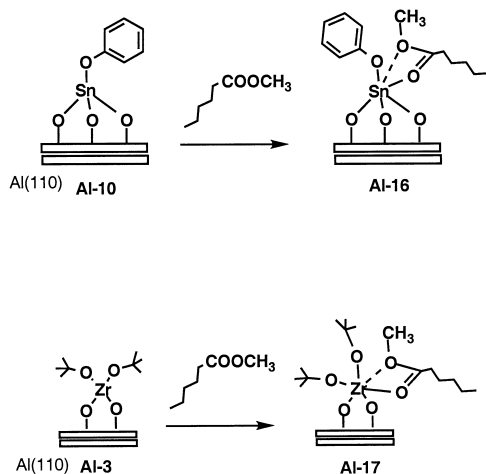Fig. 7. Metathesis from **Al-6** to give **14** and **15**.

Fig. 8. Formation of ester adducts **Al-16** and **Al-17**.

2.9. Ester adducts of Al^{110}-3 and Al^{110}-10 prepared in UHV

Surface tin complex $\mathbf{Al^{110}\text{-}10}$ (X = H) was exposed at 170 K to 0.6 L methyl caproate. FT-RAIRS analysis showed $\nu_{C=O} = 1708$ cm^{-1} and a shift in the phenoxy ligand ν_{C-O} from 1257 to 1245 cm^{-1}. These IR shifts are consistent with the tin of $\mathbf{Al^{110}\text{-}10}$ acting as a Lewis acid and with ester carbonyl group coordination as in $\mathbf{Al^{110}\text{-}16}$. Further exposure of $\mathbf{Al^{110}\text{-}16}$ to methyl caproate showed growth in the $\nu_{C=O} = 1739$ cm^{-1} peak of the ester multilayer. Similar observations were made for Zr complex $\mathbf{Al^{110}\text{-}3}$. In particular, brief exposure to methyl caproate showed $\nu_{C=O} = 1708$ cm^{-1} as in $\mathbf{Al^{110}\text{-}17}$, but it was not possible to discern any shift for the *tert*-butoxy ν_{C-O} because of ester peaks in that region of the spectrum (Fig. 8). These ester adducts may be models for carboxylic acid complexes whose formation likely preceeds ligand protonolysis [21]. FT-RAIRS analysis indicated ester adsorption was also possible onto the oxidized aluminum surface.

2.10. Transesterification catalyzed by a surface tin compound under ambient conditions

Complex **5** (5 mol% based on octanol) was dissolved in ether, and was treated with surface hydroxylated Al powder [29]; the reaction mixture was then dried in vacuo. The surface supported tin species was suspended in ethyl acetate to which 26 mmol 1-octanol was added, and the reaction mixture was stirred at room temperature. Gas chromatographic analysis after 4 h showed ca. 26% conversion to octyl acetate (ca. five turnovers); no conversion could be detected in a control reaction using just surface oxidized aluminum. We are now working to optimize tin complex-catalyzed transesterification.

3. Conclusions

We have shown that it is possible to use the techniques of UHV surface science to assist in the design of a simple catalyst for a useful organic transformation. As a bonus, UHV techniques have enabled us to elucidate details of synthesis and structure of what may be a key intermediate in the transesterification process and to infer that the catalyst species activates the ester by acting as a Lewis acid. It remains to optimize this transesterification procedure, to demonstrate its scope, and to determine the stability of the catalyst under operating reaction conditions. However, in this domain, UHV techniques will likely not be of help, and we will have to rely on less sophisticated methods of reaction development, including old fashioned chemical intuition.

References

[1] R. Imwinkelried, M. Schiess, D. Seebach, E. Vedejs, Org. Synth. 65 (1987) 230–232.
[2] A. Orita, A. Mitsutome, J. Otera, J. Org. Chem. 63 (1998) 2420–2421.

[3] J.B. Miller, S.L. Bernasek, J. Schwartz, Langmuir 10 (1994) 2629–2635.

[4] G. Lu, K.L. Purvis, J. Schwartz, S. Bernasek, Langmuir 13 (1997) 5791–5793.

[5] Y.G. Aronoff, B.L. Chen, G.C. Seto, J. Schwartz, S.L. Bernasek, J. Am. Chem. Soc. 119 (1997) 259–262.

[6] C.T. Lynch, K.S. Mazdiyasni, J.S. Smith, W.J. Crawford, Anal. Chem. 36 (1964) 2332–2337.

[7] H. Willemen, D.F. van de Vondel, G.P. van der Kelen, Inorg. Chim. Acta 34 (1979) 175180.

[8] D.T. Clark, D. Kilcast, W.K.R. Musgrave, J. Chem. Soc., Chem. Commun. (1971) 516–518.

[9] U. Gelius, P.F. Heden, J. Hedman, B.J. Lindberg, R. Manne, R. Nordberg, C. Nordling, K. Siegbahn, Phys. Scr. 2 (1970) 70–80.

[10] V.C. Simianu, J.M. Hossenlopp, Appl. Organomet. Chem. 11 (1997) 147–151.

[11] V.M. Jiménez, J.P. Espinós, A.R. González-Elipe, Surf. Sci. 366 (1996) 556–563.

[12] V.M. Jiménez, J.A. Mejías, J.P. Espinós, A.R. González-Elipe, Surf. Sci. 366 (1996) 545–555.

[13] J.F. Moulder, W.F. Stickle, P.E. Sobol, K.D. Bomben, Handbook of X-ray Photoelectron Spectroscopy, Perkin-Elmer, Physical Electronics Div., Eden Prairie, MN, 1992.

[14] L. Kövér, P.B. Barna, R. Sanjinés, Z. Kovács, G. Margaritondo, M. Adamik, Z. Radi, Thin Solid Films 90 (1996) 281–282.

[15] M. Grayson (Ed.), Kirk-Othmer Encyclopedia of Chemical Technology, Vol. 24, Wiley, New York, 1983.

[16] M. Grayson (Ed.), Kirk-Othmer Encyclopedia of Chemical Technology, Vol. 23, 3, Wiley, New York, 1983.

[17] S.K. VanderKam, G. Lu, S.L. Bernasek, J. Schwartz, J. Am. Chem. Soc. 119 (1997) 11639–11642.

[18] G. Lu, J. Schwartz, S.L. Bernasek, Langmuir 14 (1998) 1532–1534.

[19] J.B. Miller, J. Schwartz, Acta Chem. Scand. 47 (1993) 292–295.

[20] J.B. Miller, S.L. Bernasek, J. Schwartz, J. Am. Chem. Soc. 117 (1995) 4037–4041.

[21] K.L. Purvis, G. Lu, J. Schwartz, S.L. Bernasek, submitted, 1998.

[22] D.L. Allara, R.G. Nuzzo, Langmuir 1 (1985) 45–52.

[23] W.G. Golden, C.D. Snyder, B. Smith, J. Phys. Chem. 86 (1982) 4675–4678.

[24] CRC Handbook of Chemistry and Physics, Vol. 71, 1990–1991.

[25] J.P. Folkers, C.B. Gorman, P.E. Laibinis, S. Buchholz, G.M. Whitesides, R.G. Nuzzo, Langmuir 11 (1995) 813–824.

[26] P.E. Laibinis, J.J. Hickman, M.S. Wrighton, G.M. Whitesides, Science 245 (1989) 845–847.

[27] A.H.M. Sondag, M.C. Raas, J. Chem. Phys. 91 (1989) 4926–4931.

[28] J.E. Tackett, Appl. Spectrosc. 43 (1989) 483–489.

[29] J.B. Miller, J. Schwartz, S.L. Bernasek, J. Am. Chem. Soc. 115 (1993) 8239–8247.

[30] J.B. Miller, J. Schwartz, Inorg. Chem. 29 (1990) 4579–4581.

[31] F.R. Jensen, J.M. Fukoto, Acc. Chem. Res. 16 (1983) 177–184.

[32] H. Reuter, M. Kremser, Z. Anorg. Allg. Chem. 598/599 (1991) 259–268.

[33] B.A. Vaartstra, J.C. Huffman, P.S. Gradeff, L.G. Hubert-Pfalzgraf, J.-C. Daran, S. Parraud, K. Yunlu, K.G. Caulton, Inorg. Chem. 29 (1990) 3126–3131.